Infra-red collision-induced and far-line absorption in dense CO atmospheres

R. Wordsworth, F. Forget, Vincent Eymet

Accepted Manuscript

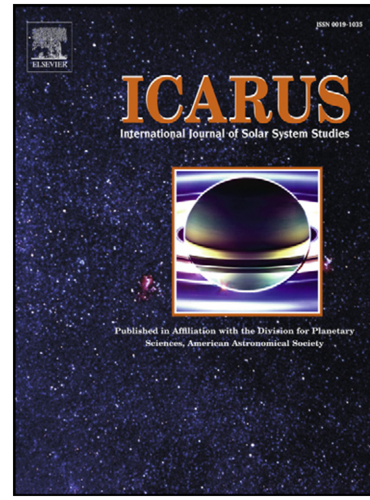

Infra-red collision-induced and far-line absorption in dense CO_2 atmospheres

R. Wordsworth, F. Forget, V. Eymet

PII: S0019-1035(10)00232-0
DOI: 10.1016/j.icarus.2010.06.010
Reference: YICAR 9462

To appear in: *Icarus*

Received Date: 16 January 2010
Revised Date: 10 June 2010
Accepted Date: 10 June 2010

Please cite this article as: Wordsworth, R., Forget, F., Eymet, V., Infra-red collision-induced and far-line absorption in dense CO_2 atmospheres, *Icarus* (2010), doi: 10.1016/j.icarus.2010.06.010

Infra-red collision-induced and far-line absorption in dense CO_2 atmospheres

R. Wordsworth [a], F. Forget [a], and V. Eymet [b]

[a] *Laboratoire de Météorologie Dynamique, Institut Pierre Simon Laplace, Paris, France.*

[b] *Laboratoire Plasma et Conversion de l'Energie, Université Paul Sabatier 118, route de Narbonne, Toulouse*

Abstract

Collision-induced absorption is of great importance to the overall radiative budget in dense CO_2-rich atmospheres, but its representation in climate models remains uncertain, mainly due to a lack of accurate experimental and theoretical data. Here we compare several parameterisations of the effect, including a new one that makes use of previously unused measurements in the 1200 to 1800 cm^{-1} spectral range. We find that a widely used parameterisation strongly overestimates absorption in pure CO_2 atmospheres compared to later results, and propose a new approach that we believe is the most accurate possible given currently available data.

Key words:

1 Introduction

Over the past few decades, the early climates of Mars, Earth and Venus have been the subject of intensive research. Of particular interest is the so-called 'early warming' problem: substantial evidence exists to suggest that liquid water was present on both Mars [Carr, 1996, Malin and Edgett, 2003, Bibring et al., 2006] and Earth [Sagan and Mullen, 1972, Appel and Moorbath, 1998, Valley et al., 2002], as long as 3.8 billion years ago. As the luminosity of the Sun at this time was likely only around 75 % of its present value [Gough, 1981], mechanisms for increased heating on both planets are necessary to explain the observations. For Mars, various hypotheses have been put forward, including transient heating events caused by meteorite impacts [Segura et al., 2002], IR scattering due to CO_2 clouds [Forget and Pierrehumbert, 1997], and volcanic emission of sulphur dioxide [Halevy et al., 2007]. All of these explanations rely in part on the presence of a thicker CO_2 atmosphere than that which exists today, and hence are sensitive to parameterisations of CO_2 continuum absorption.

In a recent study, Halevy et al. [2009] performed a detailed intercomparison of three commonly used parameterisations of dense-atmosphere CO_2 absorption using a line-by-line code. They found that the calculated outgoing longwave radiation (OLR) varied by as much as 40 W m^{-2} between total values that were of order 200 W m^{-2}, and concluded that great uncertainties remain in the radiative properties of paleoatmospheres. Clearly, better understanding of the different processes involved is required before radiative transfer in dense CO_2 atmospheres can be calculated accurately.

The physics of CO_2 absorption at high pressures is complicated by several factors. The two most important are the sublorentzian behaviour of spectral lines far from the line center, and collision-induced absorption (CIA). The latter effect is complicated and under certain conditions still poorly understood, but in simple terms, it occurs for two reasons. First, close collisions may induce transitory dipole moments in the CO_2 molecules, allowing for absorption by individual molecules in previously forbidden spectral regions. Second, in a dense gas short-lived CO_2-CO_2 dimer molecules can form. These dimers have more vibrational and rotational modes than a single CO_2 molecule, which results in the appearance of entirely new spectral absorption bands. In the thermal infrared range, the continuum effect of far lines is most important on either side of the ν_2 CO_2 15 μm (300 - 600 cm^{-1}) band, while CIA is significant between 0 and 250 cm^{-1} (induced dipole moments) and 1200 and 1500 cm^{-1} (dimer absorption) [Gruszka and Borysow, 1997, Baranov et al., 2004].

To calculate these pressure-induced opacities in climate studies involving a few bars of CO_2, such as for primitive atmospheres, the most important studies published in the past thirty years have relied without modification on a parameterisation originally derived for the Venus atmosphere by James B. Pollack [Pollack et al., 1980]. It was based on the measurements of Ho et al. [1971] from 7 to 250 cm^{-1}, and on a simple parameterisation of pressure-induced opacity in the other spectral domains described in an unpublished PhD thesis by John F. Moore [Moore, 1971, still available as a NASA report]. This parametrization included significant opacities between 295 and 526 cm^{-1} "resulting from the collision induced wings of the strong 15 μm bands". Unfortunately, this feature was kept in subsequent models, despite the fact that these opacities were probably overestimated and, in most cases, already accounted for in the codes chosen to calculate the radiative transfer in the 15 μm band (see below). This parameterisation, described in detail in Kasting et al. [1984], has been used in studies that have defined our theoretical understanding of early Mars [Pollack et al., 1987, Kasting, 1991, Forget and Pierrehumbert, 1997, Haberle, 1998, Mischna et al., 2000], the Hadean and Precambrian Earth [Kasting and Ackerman, 1986, Cadeira and Kasting, 1992, Pavlov et al., 2000, Haqq-Misra et al., 2008], the habitability of extrasolar planets [Kasting et al., 1993, Forget and Pierrehumbert, 1997] and even the terraforming of Mars [McKay et al., 1991].

In practice, the parameterisation of Kasting et al. [1984] involved an empirical equation for the CIA / far-line opacity

$$\tau_i = C_i \mathcal{W}(1 + 0.3 f_{CO_2}) \frac{p}{1 \text{ bar}} \left(\frac{T}{300 \text{ K}} \right)^{t_i} \tag{1}$$

with $\mathcal{W}$ the CO_2 path length in atmosphere-centimeters, f_{CO_2} the CO_2 mixing ratio, p the pressure in bars, T the temperature in Kelvins and C_i and t_i parameters based on experimental measurements. In a pure CO_2 atmosphere, (1) may be rewritten in terms of the absorption k_i in SI units (m^{-1}) as

$$k_i = 131.7 C_i \left(\frac{p}{101325 \text{ Pa}} \right)^2 \left(\frac{T}{300 \text{ K}} \right)^{t_i}, \tag{2}$$

where p is now in Pascals.

Although (1) has remained the standard parameterisation for the CO_2 continuum in paleoclimate studies since the 1980s, many researchers have since tackled the problems of sublorentzian line broadening and CIA, both experimentally and theoretically. For example, Perrin and Hartmann [1989], Tonkov et al. [1996], and Meadows and Crisp [1996] all studied the sublorentzian behaviour of CO_2 lines around various infrared spectral bands. In addition, Ma et al. [1999] produced a theoretical description of both the super- and sublorentzian behaviour of CO_2 spectral lines as a function of distance from the line centre. For CIA, there have also been several investigations. Tonkov et al. [1996] performed some measurements in the 2.3 μm ($\sim$4300 cm^{-1}) region, but reported large uncertainties in the values they obtained. Later, Gruszka and Borysow [1997] accurately computed the absorption due to induced-dipole effects for pure CO_2 in the 0-250 cm^{-1} spectral range. They used molecular dynamics simulations based on the $5q(CO_2)$ potential [Murthy et al., 1983] to produce absorption data for temperatures between 200 and 800 K, and proposed an analytical function to represent it. Recently, Baranov et al. [2004] also reported accurate experimental data on CO_2-CO_2 dimer absorption in the 1200-1500 cm^{-1} spectral and 193-360 K temperature ranges. They found the dependence of dimer absorption on temperature to be significantly greater than that of 'classical' induced-dipole CIA. These last two studies are particularly important for paleoclimate modelling, as together they cover all significant regions of CO_2 CIA absorption in the IR for low temperature (T_{surf} < 360 K) atmospheres.

2 Method

Although several different continuum approximations have been used in studies of Venus, early Earth and Mars, as discussed in the previous section the most common approach has been to use equation (1) combined with close line truncation (typically 10 - 50 cm^{-1}). To evaluate the errors introduced by this, we decided to compare several techniques in a simple radiative-convective climate model. We used the CIA data of Gruszka and Borysow [1997] combined with that of Baranov et al. [2004] to create a new parameterisation in the infrared, which we refer to as GBB from here for brevity. This was compared with absorption data for which no CIA was included (STD) and for which the parameterisation of Kasting et al. [1984] was used (K84). In addition, for each case we compared close (25 cm^{-1}) line truncation with untruncated data using sublorentzian line profiles. For the latter, we corrected the lorentzian lineshape using a factor $\chi(\nu - \nu_0)$, the value of which was chosen from the data of Perrin and Hartmann [1989]. We used this study because it covered a wide temperature range (190 - 800 K), and focused on the 4.3 μm ($\sim$ 2300 cm^{-1}) spectral band, which was the closest available in the 0-2000 cm^{-1} range of interest.

To examine the effects of these differences on mean atmospheric temperatures, we compared the parameterisations directly in a one-dimensional radiative-convective climate model. High resolution line-by-line spectra for a range of temperatures and pressures were computed from the *HITRAN* database [Rothman et al., 2005] using the software *kspectrum*. Kspectrum is a new program developed by one of us (V. Eymet) to accurately produce high resolution spectra for use in radiative transfer calculations. Its key advantages are that it allows one to compute the absolute error associated with any calculation for a given spectral discretisation, and that it can include the effects of far line absorption without the need for close line truncation and parameterised continuum absorption schemes. A detailed description of the program along with the source code is available online at *http://code.google.com/p/kspectrum/*.

For computational efficiency, the spectral lines were truncated at 500 cm^{-1} when sublorentzian profiles were used. This was verified to have a negligible impact on the results. For the GBB dataset, all continuum data were added directly to the high resolution spectra. The CIA data of Gruszka and Borysow [1998] were included using the code described in their paper, and the experimental results of Baranov et al. [2004] were included through linear interpolation in temperature and wavenumber. We then used the correlated-k method to compute absorption coefficients in the model. A matrix of coefficients was produced on a 6×8 temperature and log-pressure grid $T = \{100, 150, \ldots, 350\}$ K, $p = \{10^{-3}, 10^{-2}, \ldots, 10^{4}\}$ mbar. Sixteen points were used for the g-space integration, with double Gaussian spacing split at 0.95.

We used 27 spectral bands in the longwave and 7 in the shortwave. For the longwave, the band intervals used were the same as in Kasting et al. [1984]. For the calculations involving the K84 parameterisation, the continuum absorption defined in (2), which is averaged by band, was added to the total absorption after the correlated-k integration in the model.

A standard two-stream approximation was used to solve the radiative transfer equations for scattering, according to the method of Toon et al. [1989]. Rayleigh scattering was included by the method described in Hansen and Travis [1974]. For simplicity, the effects of aerosols and all other gases such as H_2O were ignored. While this allowed a clear comparison between the effects of the continuum schemes, neglecting the effect of other absorbers can increase the sensitivity of the total warming to the scheme used. We return to this point in the Discussion.

To validate the model at low pressures, we compared the total upward IR flux it produced under standard Mars conditions, for a given temperature vs. pressure profile, with line-by-line results for a pure CO_2 atmosphere [Harri et al., 2003]. We found that at all levels, the total upwards longwave radiation in the two models agreed to within 1 %. At these pressures, continuum absorption was not strong enough to affect the results.

To get an idea of the importance of the the continuum scheme to paleoclimate calculations, we also computed steady-state surface temperatures as a function of the total pressure. To reach steady-state values, we used a time-marching approach with 22 vertical levels in log-pressure coordinates. Radiative heating rates were calculated at each timestep, and in regions where CO_2 condensation occurred, the pressure and temperature were updated iteratively according to the algorithm described in Forget et al. [1998]. The solar spectrum was multiplied by 0.75 to approximate the effect of the weaker early Sun, and the visible surface albedo was set to $A_s = 0.2$. The total flux was divided by two to account for diurnal averaging and the solar zenith angle θ_z was set to 60°. As this simple model does not include the effects of absorption by other gases or by aerosols, the values of T_{surf} reached were well below 273 K even at the maximum surface pressure studied (5 bar).

In the lower troposphere, the temperature was varied according to the ideal gas lapse rate $\Gamma = -g/c_p$, with $c_p = 735.82$ J kg^{-1} K^{-1} a constant. This introduced a small error due to the fact that CO_2 behaves non-ideally at high pressures and low temperatures. As a) we did not perform calculations at surface pressures greater than 5 bar and b) our primary objective was a comparison among the various CIA parameterisations under the same conditions, the error introduced by this approximation is not important to the main result. The temperature profile in the upper troposphere was controlled by CO_2 condensation, and the radiative effects of CO_2 cloud formation were not considered.

Finally, for the OLR calculations (Figure 2) the same fixed temperature profile was used in each case. A surface temperature of 250 K was chosen, and the profile in the atmosphere was determined using a method similar to that of Kasting [1991]. The stratosphere for these cases was set to be isothermal with temperature 167 K.

3 Results

In Figure 1a), the total absorption in a 1-bar, 273-K pure CO_2 gas between 0 and 2000 cm^{-1} is plotted, with the regions of induced dipole and dimer absorption clearly indicated. In Figure 1b), equation (2) (K84) is plotted against the new CIA data (GBB), for three different gas temperatures. As the absorption in both CIA parameterisations increased with the square of pressure, we focus on the variation with temperature here. As can be seen, the results roughly agree over most of the spectral range. However, the increase of (2) with temperature is slightly more rapid. More critically, there is a small but important region between 250 and 500 cm^{-1} where (2) predicts anomalously large absorption. As will be seen, this latter effect in particular can cause large differences in the resultant surface temperature in one-dimensional climate calculations.

In Fig. 2, the outgoing longwave radiation (OLR) from an example 2-bar atmosphere with surface temperature of 250 K is shown as a function of wavenumber, for the STD (a), K84 (b) and GBB (c) parameterisations. For each case, the effects of 25 cm^{-1} truncation and sublorentzian line profiles are also shown. As may be seen, truncation (dashed lines) has the predictable effect of narrowing the main 660 cm^{-1} (15 μm) CO_2 vibrational absorption band, allowing the escape of a significant amount of radiation in that spectral region that would otherwise have been absorbed. The CIA also has an important effect at this pressure, decreasing the outgoing flux in the regions below 500 cm^{-1} and above 1100 cm^{-1}. However, there are significant differences between the GBB and K84 schemes, with the latter causing a greater reduction in the OLR at all wavenumbers. In particular, the anomalous absorption of K84 in the 250 to 500 cm^{-1} region greatly decreases the outgoing flux there. The severity of the effect is increased because it occurs close to the peak of the blackbody spectrum ($\sim$ 490 cm^{-1} for a surface temperature T_s=250 K).

To get an idea of the importance of these differences in paleoclimate calculations, we next computed steady-state surface temperatures as a function of the surface pressure. Figure 3 shows the results for the STD (a), K84 (b) and GBB (c) parameterisations. Here dashed and solid lines indicate 25 cm^{-1} truncation and sublorentzian line profiles, as before. As can be seen, the agreement between all parameterisations is close for pressures below a few tenths of a bar. This demonstrates that the effects of continuum absorption are negligible there. As in Kasting [1991], in each case T_{surf} increases to a maximum for $p_{surf} \sim$ a few bar and then decreases, due to the effects of both CO_2 condensation and Rayleigh scattering. However, the values diverge seriously at high pressures, with the K84 parameterisation predicting a maximum surface temperature of around 240 K, compared with 220 K and 210 K for GBB and STD, respectively. Line truncation also has a significant effect on the results in each case, decreasing the maximum surface temperature by between 7 K (for STD) and 25 K (for K84).

In Figure 4, we have plotted the difference between surface temperatures using the K84 scheme with truncation (dashed line in Fig. 3b) and the GBB scheme with sublorentzian line profiles (solid line in Fig. 3c). These two schemes were compared because the former is widely used in paleoclimate research, while we believe that the latter is the most physically accurate (we return to this point in the conclusion). As can be seen, while the truncated K84 scheme causes slightly decreased warming at low surface pressures, it overestimates the equilibrium surface temperature at 2-3 bars by almost 10 K. This occurs primarily because the errors inherent in the K84 scheme due to line truncation are overcompensated by the absorption described by (1) between 250 and 500 cm^{-1}.

4 Discussion

In agreement with Halevy et al. [2009], our results indicate that the choice of continuum parameterisation greatly influences the radiative balance in CO_2-rich atmospheres. While they did not make any conclusions as to the absolute accuracy of the various schemes used, we have combined the most accurate CIA and sublorentzian data currently available to show that the parameterisations used most frequently in the literature are likely to strongly *overestimate* the total longwave absorption caused by the continuum, chiefly due to increased absorption in the 250-500 cm^{-1} spectral region. Clearly, these results have important consequences for the 'faint young Sun' problem. All previous studies that used the K84 / line truncation parameterisation should unfortunately be regarded as overestimating the total surface warming.

How confident can we be of the absolute accuracy of the GBB + sublorentzian line profile parameterisation? For the CIA, both the results of Baranov et al. [2004] and Gruszka and Borysow [1997] appear robust. Baranov et al. [2004] compared their experimental results with several previous studies, and found them to be in broad agreement, although the spectral resolution and overall accuracy in their results were greater. As noted previously, Gruszka and

Borysow [1997] was a purely theoretical study. However they compared their predictions with previous experimental results (principally Ho et al. [1971]), and found close agreement over the entire temperature range of the experiments (233 - 400 K).

The sublorentzian parameterisation is a little more uncertain, as no studies currently exist of far-line profiles near the 15 μm band. However, studies such as Tonkov et al. [1996] yielded results close to those of Perrin and Hartmann [1989] (see e.g., Fig. 1 in Halevy et al. [2009]).This at least suggests that the sublorentzian behaviour around the 15 μm band is also similar. To improve the accuracy of dense CO_2 opacity calculations in the future, we suggest that it would be useful to perform precise direct measurements of the sublorentzian profiles in this region.

An additional subtlety occurs because existing sublorentzian parameterisations are inaccurate close to the line centers, where the profile is typically superlorentzian. Ma et al. [1999] used a fairly advanced theoretical model to compute line shapes in IR CO_2 bands accurately as a function of temperature and spectral range. For the intensive line-by-line computations required for climate studies, however, their model is unfortunately still too complex. An assessment of the importance of this effect in the overall radiative budget of dense atmospheres could be a subject of future study. However, at high pressures the main CO_2 absorption bands are already fully saturated, so its parameterisation should be less critical than the effects we have investigated here.

The extent to which the total warming is affected by continuum absorption will clearly depend on the contribution of other effects to the radiative balance. Here we have only considered pure CO_2 atmospheres without other gases or aerosols. As noted by Halevy et al. [2009], the effect of other greenhouse gases is generally to decrease the sensitivity of climate calculations to the parameterisation used for CO_2 CIA. H_2O, in particular, absorbs quite strongly in the 250-500 cm^{-1} region, which we identified earlier as the part of the spectrum where the difference between K84 and GBB was the most important. Thus broadly speaking for an extremely wet atmosphere, as may have been the case for early Venus and/or Earth, the differences we have described here may not be critical to the climate. For early Mars, in contrast, the difference is important, as even in the most optimistic climate scenarios, global mean surface temperatures are seldom much greater than 0°C, and hence the atmosphere is relatively dry. In addition, these results may have implications for radiative transfer studies of present-day Venus and, potentially, of exoplanet atmospheres.

Hence despite the caveats just mentioned, for future studies of dense CO_2 atmospheres we suggest that the GBB parameterisation described here, in combination with sublorentzian line profiles based on the results of Perrin and Hartmann [1989], offers the highest accuracy available until further experimental or theoretical studies are performed. For ease of use in future climate calculations, we have made a *Fortran* routine to compute the GBB parameterisation available online at *http://code.google.com/p/kspectrum/*.

Acknowledgements

We would like to thank Bob Haberle for providing us with a radiative transfer code that formed the basis of the correlated-k scheme used in this study, and the authors of Baranov et al. [2004] for allowing us to use their experimental data directly in our spectral calculations. R. Wordsworth acknowledges funding from l'Institut de France, Fondation Cino et Simone Del Duca.

References

F. Appel and M. Moorbath. Recognizable primary volcanic and sedimentary features in a low-strain domain of the highly deformed, oldest known (3.8 Gyr) Greenstone Belt, Isua, West Greenland. *Terra Nova*, 10:57–62, 1998.

Y. I. Baranov, W. J. Lafferty, and G. T. Fraser. Infrared spectrum of the continuum and dimer absorption in the vicinity of the O2 vibrational fundamental in O2/CO2 mixtures. *Journal of Molecular Spectroscopy*, 228: 432–440, December 2004. doi: 10.1016/j.jms.2004.04.010.

J.-P. Bibring, Y. Langevin, J. F. Mustard, F. Poulet, R. Arvidson, A. Gendrin, B. Gondet, N. Mangold, P. Pinet, and F. Forget. Global Mineralogical and Aqueous Mars History Derived from OMEGA/Mars Express Data. *Science*, 312:400–404, 2006. doi: 10.1126/science.1122659.

K. Cadeira and J. F Kasting. Susceptibility of the early earth to irreversible glaciation caused by carbon dioxide clouds. *Nature*, 359:226–228, 1992.

M. H. Carr. *Water on Mars.* New York: Oxford University Press, —c1996, 1996.

F. Forget and R. T. Pierrehumbert. Warming Early Mars with Carbon Dioxide Clouds That Scatter Infrared Radiation. *Science*, 278:1273–1276, November 1997.

F. Forget, F. Hourdin, and O. Talagrand. CO2 Snowfall on Mars: Simulation with a General Circulation Model. *Icarus*, 131:302–316, February 1998. doi: 10.1006/icar.1997.5874.

D. O. Gough. Solar interior structure and luminosity variations. *Solar Physics*, 74:21–34, November 1981.

M. Gruszka and A. Borysow. Roto-Translational Collision-Induced Absorption of CO2 for the Atmosphere of Venus at Frequencies from 0 to 250 cmˆ-1,

at Temperatures from 200 to 800 K. *Icarus*, 129:172–177, September 1997. doi: 10.1006/icar.1997.5773.

M. Gruszka and A. Borysow. Computer simulation of the far infrared collision induced absorption spectra of gaseous CO2. *Molecular Physics*, 93:1007–1016, 1998. doi: 10.1080/002689798168709.

R. M. Haberle. Early Mars climate models. 103:28467, 1998.

I. Halevy, M. T. Zuber, and D. P. Schrag. A Sulfur Dioxide Climate Feedback on Early Mars. *Science*, 318:1903–1907, December 2007. doi: 10.1126/science.1147039.

I. Halevy, R. T. Pierrehumbert, and D. P Schrag. Radiative transfer in CO2-rich paleoatmospheres. *Journal of Geophysical Research (Atmospheres)*, 114, September 2009. doi: 10.1029/2009JD011915.

J. E. Hansen and L. D. Travis. Light scattering in planetary atmospheres. *Space Science Reviews*, 16:527–610, October 1974. doi: 10.1007/BF00168069.

J. D. Haqq-Misra, S. D. Domagal-Goldman, P. J. Kasting, and J. F. Kasting. A Revised, Hazy Methane Greenhouse for the Archean Earth. *Astrobiology*, 8:1127–1137, 2008. doi: 10.1089/ast.2007.0197.

A.-M. Harri, D. Crisp, and H. Savijärvi. Intercomparison of Atmospheric Radiation Schemes for the Lower Martian Atmosphere. In A. L. Albee & H. H. Kieffer, editor, *Sixth International Conference on Mars*, pages 3089–+, July 2003.

W. Ho, G. Birnbaum, and A. Rosenberg. Far-Infrared Collision-Induced Absorption in CO2. I. Temperature Dependence. *Journal of Chemical Physics*, 55:1028–1038, August 1971. doi: 10.1063/1.1676181.

J. F. Kasting. CO2 condensation and the climate of early Mars. *Icarus*, 94: 1–13, November 1991. doi: 10.1016/0019-1035(91)90137-I.

J. F. Kasting and T. P. Ackerman. Climatic consequences of very high carbon dioxide levels in the earth's early atmosphere. *Science*, 234:1383–1385, 1986. doi: 10.1126/science.11539665.

J. F. Kasting, J. B. Pollack, and D. Crisp. Effects of high CO2 levels on surface temperature and atmospheric oxidation state of the early earth. *Journal of Atmospheric Chemistry*, 1:403–428, 1984.

J. F. Kasting, D. P. Whitmire, and R. T. Reynolds. Habitable Zones around Main Sequence Stars. *Icarus*, 101:108–128, January 1993. doi: 10.1006/icar.1993.1010.

Qiancheng Ma, Richard H. Tipping, Christian Boulet, and Jean-Pierre Bouanich. Theoretical Far-Wing Line Shape and Absorption for High-Temperature CO2. *Appl. Opt.*, 38(3):599–604, 1999. URL `http://ao.osa.org/abstract.cfm?URI=ao-38-3-599`.

M. C. Malin and K. S. Edgett. Evidence for Persistent Flow and Aqueous Sedimentation on Early Mars. *Science*, 302:1931–1934, 2003.

C. P. McKay, O. B. Toon, and J. F. Kasting. Making Mars habitable. *Nature*, 352:489–496, 1991. doi: 10.1038/352489a0.

V. S. Meadows and D. Crisp. Ground-based near-infrared observations of the Venus nightside: The thermal structure and water abundance near the surface. *Journal of Geophysical Research (Planets)*, 101:4595–4622, 1996. doi: 10.1029/95JE03567.

M. A. Mischna, J. F. Kasting, A. Pavlov, and R. Freedman. Influence of carbon dioxide clouds on early martian climate. *Icarus*, 145:546–554, 2000. doi: 10.1006/icar.2000.6380.

J. F. Moore. Infrared absorption of carbon dioxide at high densities with application to the atmosphere of Venus. Technical Report X-630-72-48, NASA Goddard Space Flight Center, Greenbelt, Md, 1971.

C. S. Murthy, S. F. O'Shea, and I. R. McDonald. Electrostatic interactions in molecular crystals. *Molecular Physics*, 50:531–541, October 1983. doi: 10.1080/00268978300102531.

A. A. Pavlov, J. F. Kasting, L. L. Brown, K. A. Rages, and R. Freedman. Greenhouse warming by CH4 in the atmosphere of early Earth. *J. Geophys. Res.*, 105:11981–11990, 2000. doi: 10.1029/1999JE001134.

M. Y. Perrin and J. M. Hartmann. Temperature-dependent measurements and modeling of absorption by CO2-N2 mixtures in the far line-wings of the 4.3-micron CO2 band. *Journal of Quantitative Spectroscopy and Radiative Transfer*, 42:311–317, October 1989. doi: 10.1016/0022-4073(89)90077-0.

J. B. Pollack, O. B. Toon, and R. Boese. Greenhouse models of Venus' high surface temperature, as constrained by Pioneer Venus measurements. *J. Geophys. Res.*, 85:8223–8231, 1980. doi: 10.1029/JA085iA13p08223.

J. B. Pollack, J. F. Kasting, S. M. Richardson, and K. Poliakoff. The case for a wet, warm climate on early Mars. *Icarus*, 71:203–224, 1987.

L. S. Rothman, D. Jacquemart, A. Barbe, D. Chris Benner, M. Birk, L. R. Brown, M. R. Carleer, C. Chackerian, K. Chance, L. H. Coudert, V. Dana, V. M. Devi, J.-M. Flaud, R. R. Gamache, A. Goldman, J.-M. Hartmann, K. W. Jucks, A. G. Maki, J.-Y. Mandin, S. T. Massie, J. Orphal, A. Perrin, C. P. Rinsland, M. A. H. Smith, J. Tennyson, R. N. Tolchenov, R. A. Toth, J. Vander Auwera, P. Varanasi, and G. Wagner. The HITRAN 2004 molecular spectroscopic database. *Journal of Quantitative Spectroscopy and Radiative Transfer*, 96:139–204, December 2005. doi: 10.1016/j.jqsrt.2004.10.008.

C. Sagan and G. Mullen. Earth and Mars: Evolution of Atmospheres and Surface Temperatures. *Science*, 177:52–56, 1972. doi: 10.1126/science.177.4043.52.

T. L. Segura, O. B. Toon, A. Colaprete, and K. Zahnle. Environmental Effects of Large Impacts on Mars. *Science*, 298:1977–1980, December 2002. doi: 10.1126/science.1073586.

M. V. Tonkov, N. N. Filippov, V. V. Bertsev, J. P. Bouanich, N. van-Thanh, C. Brodbeck, J. M. Hartmann, C. Boulet, F. Thibault, and R. Le Doucen. Measurements and empirical modeling of pure CO2 absorption in the 2.3- m region at room temperature: far wings, allowed and collision-induced bands. *Applied Optics*, 35:4863–4870, August 1996.

O. B. Toon, C. P. McKay, T. P. Ackerman, and K. Santhanam. Rapid calculation of radiative heating rates and photodissociation rates in inhomogeneous multiple scattering atmospheres. *Journal of Geophysical Research*, 94:16287–16301, November 1989. doi: 10.1029/JD094iD13p16287.

J. W. Valley, W. H. Peck, E. M. King, and S. A. Wilde. A cool early Earth. *Geology*, 30:351, April 2002. doi: 10.1130/0091-7613(2002)030.

Fig. 1. a) Total longwave absorption in a pure CO_2 gas at 1 bar and 273 K. b) Comparison of the CIA absorption shown in a) (GBB; black lines) with the parameterisation of Kasting et al. [1984] (K84; filled circles). As can be seen, the difference between the two datasets is extremely large in the 250 - 500 cm^{-1} region.

Fig. 2. Outgoing longwave radiation (OLR) from a 2-bar pure CO_2 atmosphere of surface temperature 250 K and vertical temperature profile as described in the text. The CIA parameterisations used were a) STD (no CIA), b) K84 and c) GBB. In each case the dotted line indicates the (blackbody) OLR when the atmospheric absorption is zero, while the dashed and solid lines indicate the OLR when the absorption is calculated with line truncation at 25 cm^{-1} and with the sublorentzian profiles of Perrin and Hartman (1989), respectively.

Fig. 3. Surface pressure vs. surface temperature for the STD (a), K84 (b) and GBB (c) parameterisations. As in Figure 2, solid and dashed lines show results with sublorentzian far-line profiles and with 25 cm^{-1} line truncation, respectively. The dotted line is the CO_2 vapour-pressure curve.

Fig. 4. Surface pressure vs. surface temperature difference between the K84 pameterisation with 25 cm^{-1} line truncation (dashed line in Fig. 3b) and the GBB pameterisation with sublorentzian line profiles (solid line in Fig. 3c).

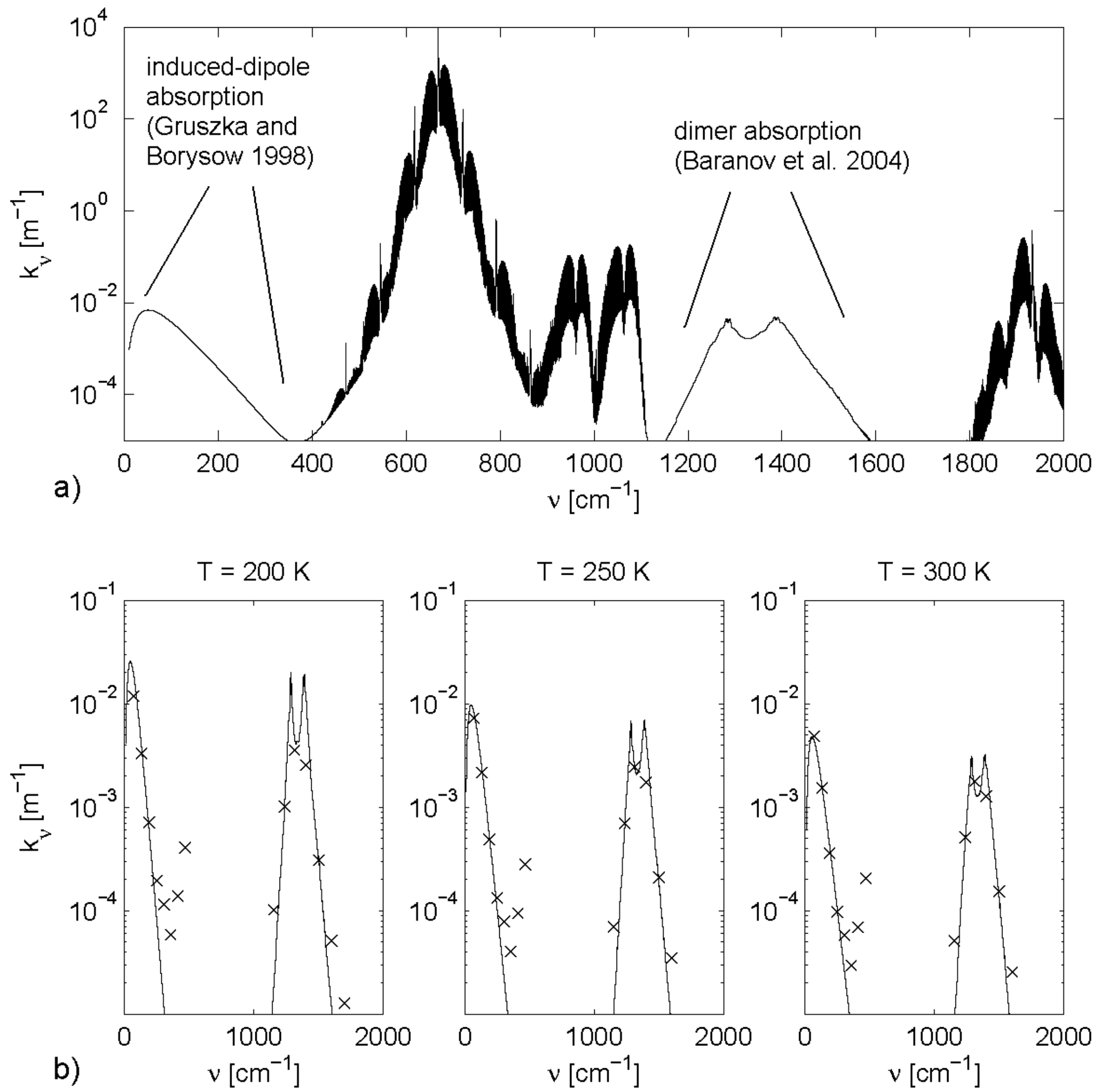
induced-dipole absorption (Gruszka and Borysow 1998)
dimer absorption (Baranov et al. 2004)
k_ν [m^{-1}]
ν [cm^{-1}]
a)
T = 200 K
T = 250 K
T = 300 K
b)

Fig1

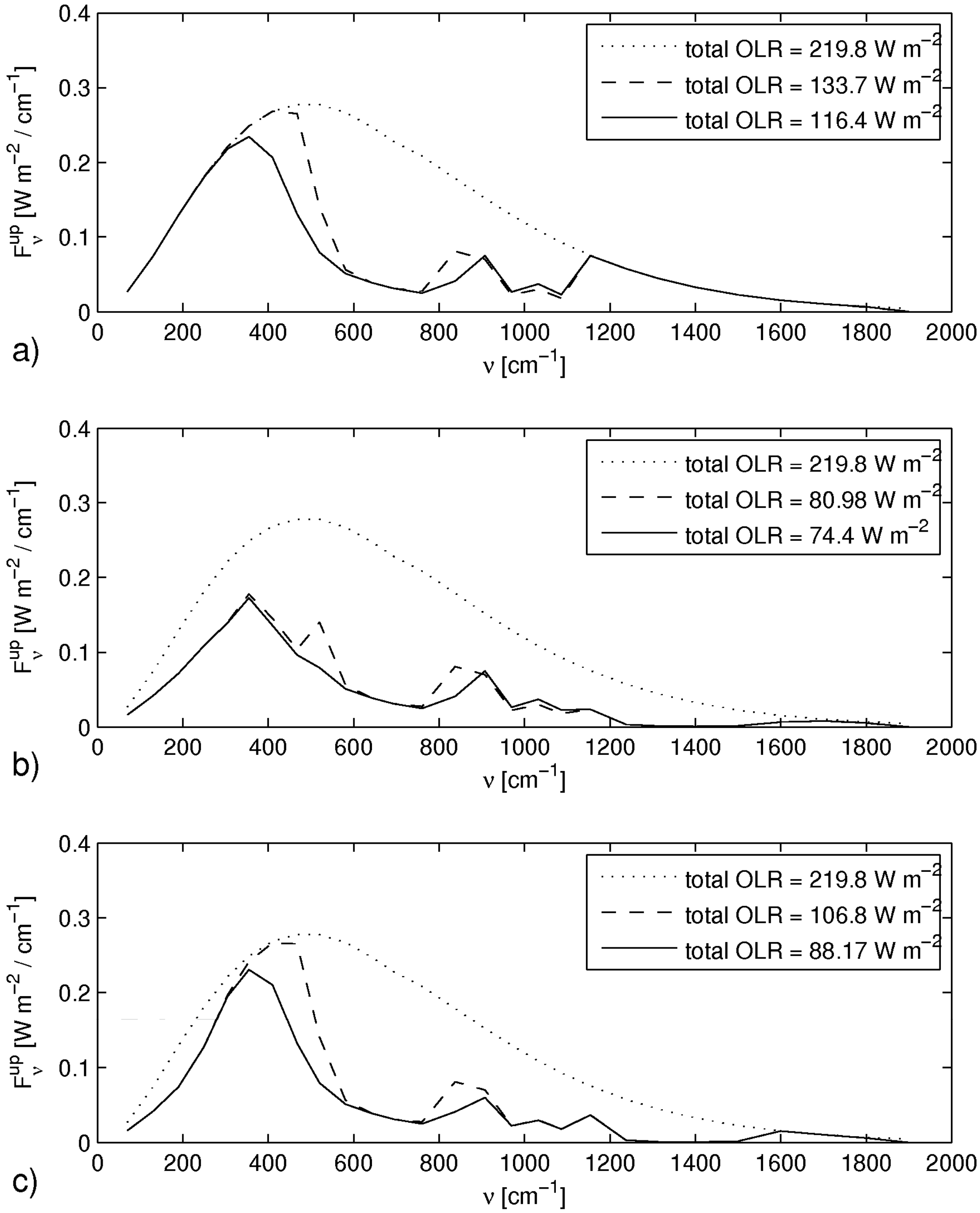
total OLR = 219.8 W m^{-2}
total OLR = 133.7 W m^{-2}
total OLR = 116.4 W m^{-2}
F_ν^{up} [W m^{-2} / cm^{-1}]
ν [cm^{-1}]
a)
total OLR = 219.8 W m^{-2}
total OLR = 80.98 W m^{-2}
total OLR = 74.4 W m^{-2}
F_ν^{up} [W m^{-2} / cm^{-1}]
ν [cm^{-1}]
b)
total OLR = 219.8 W m^{-2}
total OLR = 106.8 W m^{-2}
total OLR = 88.17 W m^{-2}
F_ν^{up} [W m^{-2} / cm^{-1}]
ν [cm^{-1}]
c)

Fig2

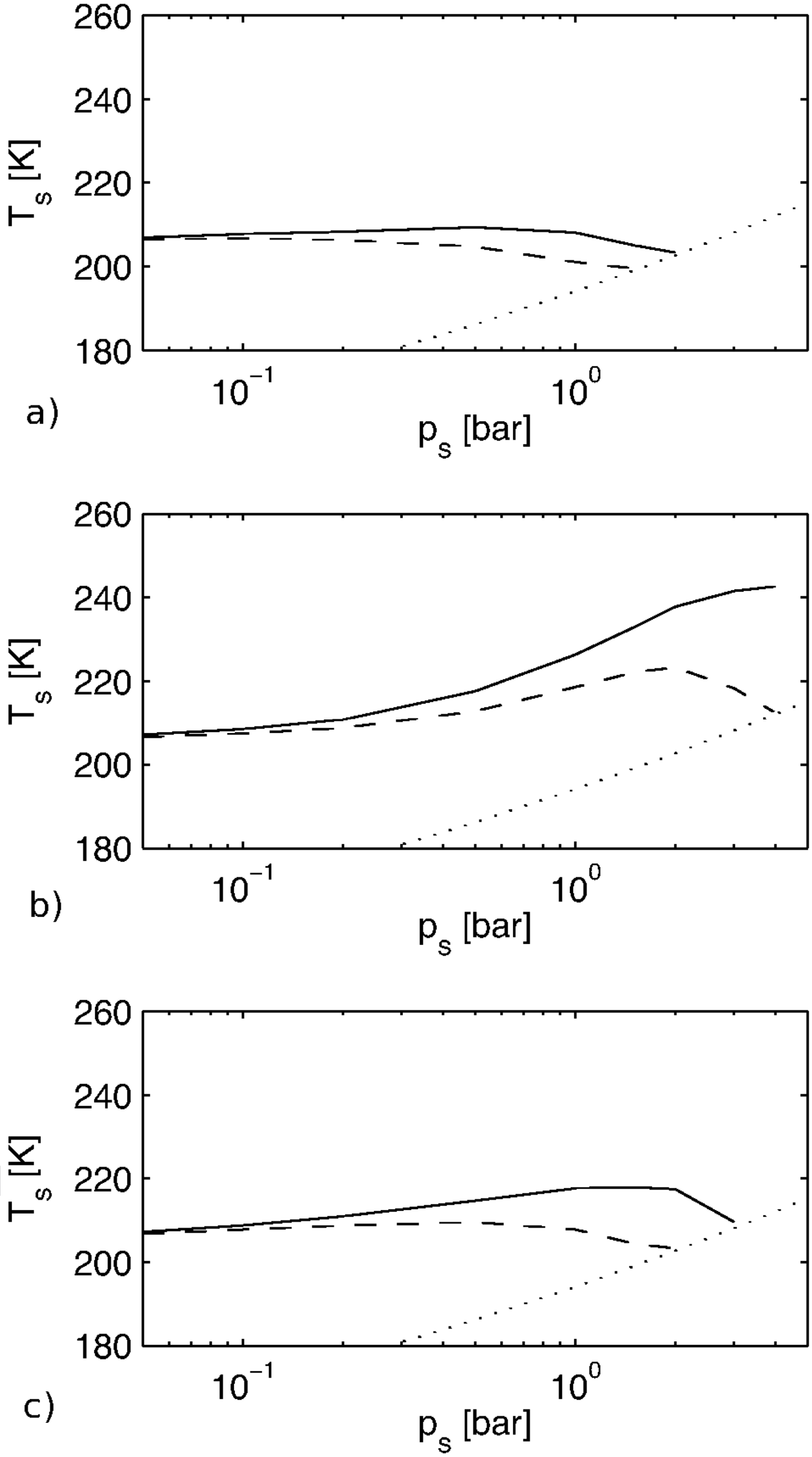

260
240
220
200
180
T_s [K]
10^{-1}
10^{0}
p_s [bar]
a)
b)
c)

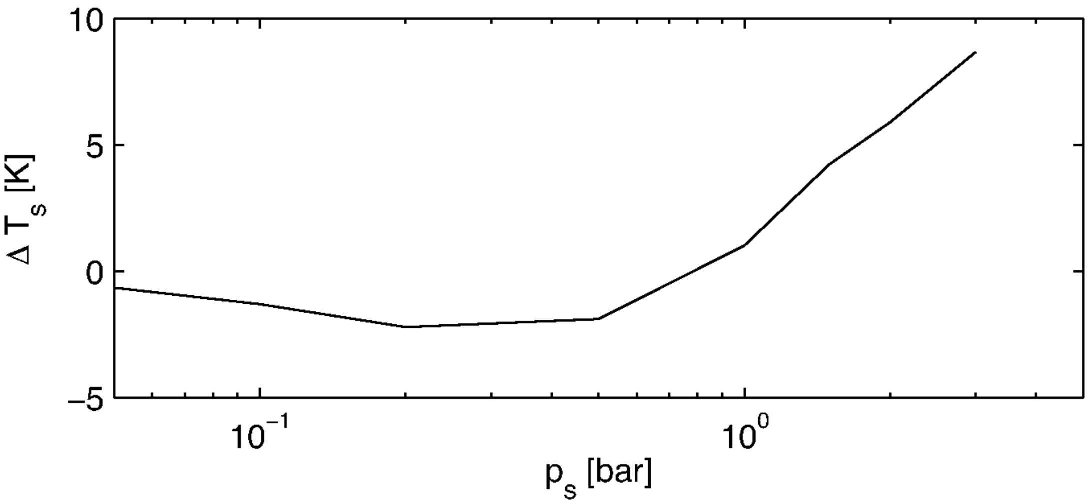

Fig4